Brief Communication

# Effect of fuel nozzle material properties on soot formation and temperature field in coflow laminar diffusion flames

Ömer L. Gülder [a,*], Kevin A. Thomson [b], David R. Snelling [b]

[a] *Institute for Aerospace Studies, University of Toronto, 4925 Dufferin Street, Toronto, Ontario M3H 5T6, Canada*
[b] *ICPET Combustion Technology, National Research Council, 1200 Montreal Road M-9, Ottawa, Ontario K1A 0R6, Canada*

## 1. Introduction

Laminar coflow diffusion flames are very sensitive to initial conditions and perturbations [1–4]. Although coflow flames are 2-D, there has been a considerable effort for modeling these flames with detailed chemical kinetics [5–7] and with skeletal kinetic mechanisms [8,9]. These modeling efforts and comparisons among coflow burners of similar geometries require consistent and well-defined initial conditions. One of these is the properties of the material used for the fuel tube.

The influence of the properties of the fuel tube on soot formation was noted by Kent and Wagner [2]. They placed a small glass ring, 5 mm high, on the water-cooled metal tube to reduce the heat transfer rate. They noted that, at low fuel flow rates, a non-smoking flame was transformed to a smoking one. They found that at higher fuel flow rates the effect of the glass ring is minimal [2]. Although they did not provide detailed results and discussions, they noted up to a 100 K temperature increase on the centerline of the flame at 5 mm above the burner rim with the glass ring.

In the present study, we investigated the influence of fuel tube material (i.e., steel, aluminum, and Pyrex glass) thermal properties on soot formation, and the temperature field of laminar coflow diffusion flames.

The spatially resolved soot volume fractions and soot surface temperatures were determined from tomographic reconstruction of spectrally resolved radiation from soot particles.

## 2. Experimental methodology

We used soot spectral emission spectroscopy to measure soot temperature and volume fraction. The experimental setup and the measurement technique are described in detail previously [10]. A brief summary will be given here. Radiation emission from soot in the laminar diffusion flame passed through an adjustable aperture and was focused by a 104-mm-diameter achromatic lens onto the entrance slit of a spectrometer. The spectrometer slit was oriented vertically with a height of 0.5 mm and a width of 0.025 mm. The output from the spectrometer was imaged onto a CCD detector. The optics were set for 1:1 imaging magnification.

The three laminar diffusion flame burners we used are duplicates of the burner previously reported by the current authors [10,11]. The only difference is the material used for the burner tube (steel, aluminum, or Pyrex glass). Each burner consists of a 10.9-mm-inner-diameter fuel tube, centered in a 100-mm-diameter air nozzle. The air passes through packed beds of glass beads and porous metal disks to smooth the flow and prevent flame instabilities. The ethylene flow rate was $3.23 \times 10^{-6}$ m$^3$/s and that of propylene was $0.667 \times 10^{-6}$ m$^3$/s (at 21 °C and 1 atm),

---

* Corresponding author. Fax: +1 416 667 7721.
  *E-mail address:* omer.gulder@utoronto.ca
(Ö.L. Gülder).

| | | T/C1 | T/C2 |
|---|---|---|---|
| Al | P | 100 | 90 |
| | E | 120 | 104 |
| Steel | P | 115 | 102 |
| | E | 124 | 98 |
| Glass | P | 106 | 37 |
| | E | 119 | 41 |

Temperature, °C

P = propylene
E = ethylene
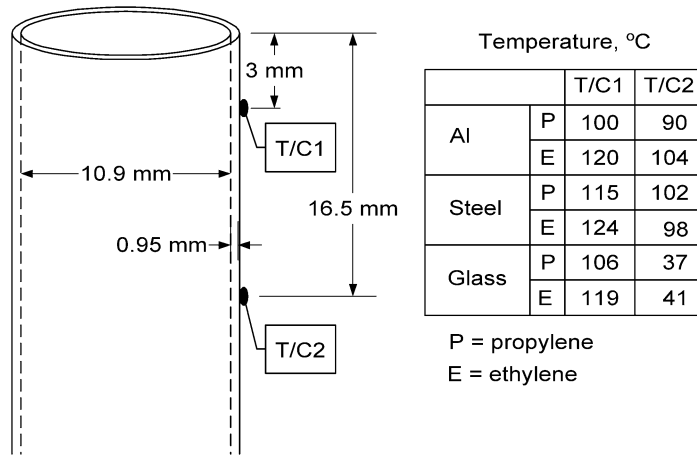
Fig. 1. Dimensions of the fuel nozzle tube and locations of the thermocouples (T/C1 and T/C2). Fuel nozzle outer surface temperatures are listed in the table.

whereas the air coflow was $4.73 \times 10^{-3}$ m$^3$/s. Under these flow conditions and with steel fuel nozzles, both fuels provided overventilated laminar diffusion flames burning slightly under their smoke points; that is, no soot escaped from the tip of the flame. The flame structure seemed to be insensitive to air flow rate; however, the chosen air flow rate provided the most stable flames free from flickering. A flame enclosure made of flexible steel mesh protected the flame from air movements in the room. An appropriate viewing port in the mesh provided optical access. The burner being used was attached to a positioning platform with accurate and repeatable positioning both vertically and horizontally. Fuel nozzle surface temperatures were measured by thermocouples. Dimensions of the fuel nozzle and the location of the thermocouple measurements are shown in Fig. 1.

Horizontal scans of line integrated spectra were collected over a spectral range from 500 to 945 nm. Each data acquisition consisted of a spectrum averaged from five 1-s exposures. The spectral images were summed vertically over the 0.5-mm slit height to improve the signal to noise ratio. The spectra were also binned horizontally (spectrally) into 25-nm bins. The spectrometer was calibrated with a tungsten strip filament lamp, placed coincident with the burner center and of known brightness temperature. The filament lamp was calibrated against a secondary standard photoelectric pyrometer at a wavelength of 649 nm. Further details are given in [10].

## 3. Results and discussion

The one-dimensional tomography was performed on the data using a three-point Abel inversion method [11]. In tomographic inversion, it is as-

sumed that the property being measured is essentially constant over the cross-sectional area sampled, and that all regions along the optical axis are sampled equally. For practical line-of-sight measurements, the sampling cross section changes with position along the measurement chord. In addition, flame emission is attenuated through self-absorption while passing through the flame. Strictly speaking, this means that emission measurements are not line integrals of a local property field as is required for tomographic reconstruction. These two concerns are addressed in detail elsewhere [10].

Fig. 2 shows the temperature profiles calculated as described in [10] with and without radiation extinction taken into account in the ethylene flame. These temperature profiles are compared in Fig. 2 to temperatures measured by CARS nitrogen thermometry in the same flame. CARS measurements of temperatures in ethylene flame on the steel burner were described previously [12]. Error bars on CARS data indicate the precision of the measurements and are about 50 K. Soot surface temperature data with and without radiation extinction correction do not show any significant difference, especially at higher radial locations. The maximum difference, about 20 K, seems to be largest around the flame centerline at this axial location of 30 mm downstream. Similar agreements were obtained at 10 and 20 mm downstream locations where CARS data were available [12].

Also shown in Fig. 2 is the absorption coefficient, from which soot volume fraction can be calculated [10]. The absorption coefficient data are compared to absorption coefficients obtained by 2-D imaging on the same burner [13]. The agreement is good except at the peak. The peak value measured by radiation emission spectroscopy is higher by about 10% than 2-D extinction measurements possibly due
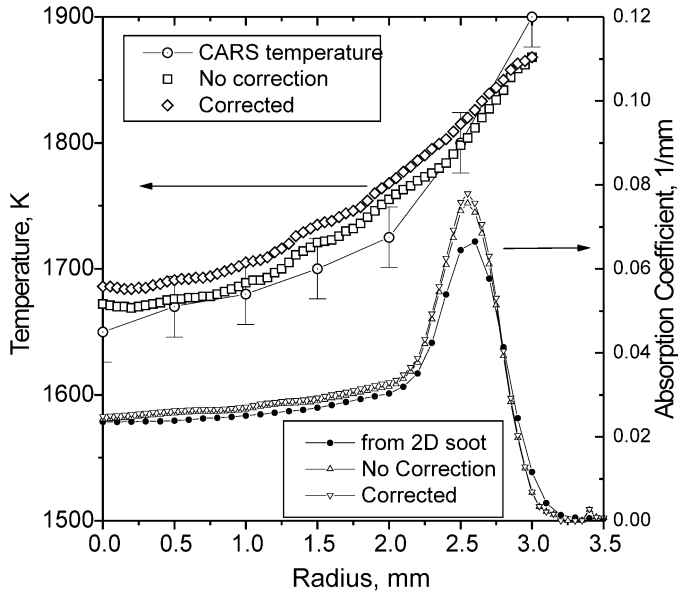
Fig. 2. Comparison of the soot surface temperatures obtained from emission spectroscopy with and without extinction correction to CARS temperature measurements made on the same burner [11]. Also shown is the comparison of the soot absorption coefficient data (with and without extinction correction) obtained in this work to absorption coefficients measured by 2-D imaging [13].

to the finer effective spatial resolution of the former. Absorption coefficient data with and without radiation extinction correction do not show any significant difference (Fig. 2).

### 3.1. Propylene flames

Radial soot volume fractions of the propylene flames with three different burner materials are shown in Fig. 3, for downstream locations of 4, 6, and 8 mm, and in Fig. 4, for downstream locations of 10, 12, 14, 16, and 18 mm. At lower downstream locations (Fig. 3), soot concentrations produced by the glass fuel nozzle are much higher than those with the aluminum and steel nozzles. Peak soot concentrations of the glass nozzle are 70–80% higher than those of the aluminum nozzle, whereas the soot concentrations of the steel nozzle flame are 17–28% higher than those of the aluminum nozzle. Similar concentration differences are observed at higher heights as shown in Fig. 4. At the chosen flow rate of propylene, the diffusion flames on aluminum and steel nozzles burn slightly under the smoke point height. However, with the glass burner at the same fuel flow rate, the propylene flame burns above its smoke point and soot escapes from the tip of the flame (inset in Fig. 3).

Radial profiles of the soot surface temperatures are shown in Fig. 5, for downstream locations of 4, 6, and 8 mm, and in Fig. 6, for downstream locations of 12, 14, 16, and 18 mm. At all downstream loca-

tions, soot surface temperatures of the glass nozzle flame are consistently lower than those of the aluminum and steel nozzle flames. At lower locations the differences are about 25 to 80 K at radial distances larger than 1 mm (Fig. 5). At higher downstream locations differences in temperature grow toward the tip of the flame and at the 18-mm plane, the difference is about 200–250 K (Fig. 6). The soot surface temperatures of the aluminum nozzle flame are slightly higher than those of steel nozzle throughout the flame (Figs. 5 and 6).

The observed behavior of the soot concentrations and soot surface temperatures can be explained in terms of the thermal conductivities and emissivities of the fuel nozzle materials. The flame heats up the fuel nozzle by conduction and, to a limited extent, by radiation. In turn, the fuel nozzle dissipates this heat by conduction along an axial upstream direction while, at the same time, transferring some of it to the fuel stream by convection inside the nozzle and to the air stream adjacent to the outside of the fuel nozzle, effectively raising the temperatures of reactant gases. The ratio of heat dissipated by conduction to heat transferred to the reactant gases is dependent on the thermal diffusivity of the nozzle material. Thermal diffusivity of aluminum is about 9 times higher than that of steel, and about 250 times higher than that of glass [14]. Therefore, steel and aluminum fuel nozzles dissipate heat by conduction faster than it is convected to the reactant gases.
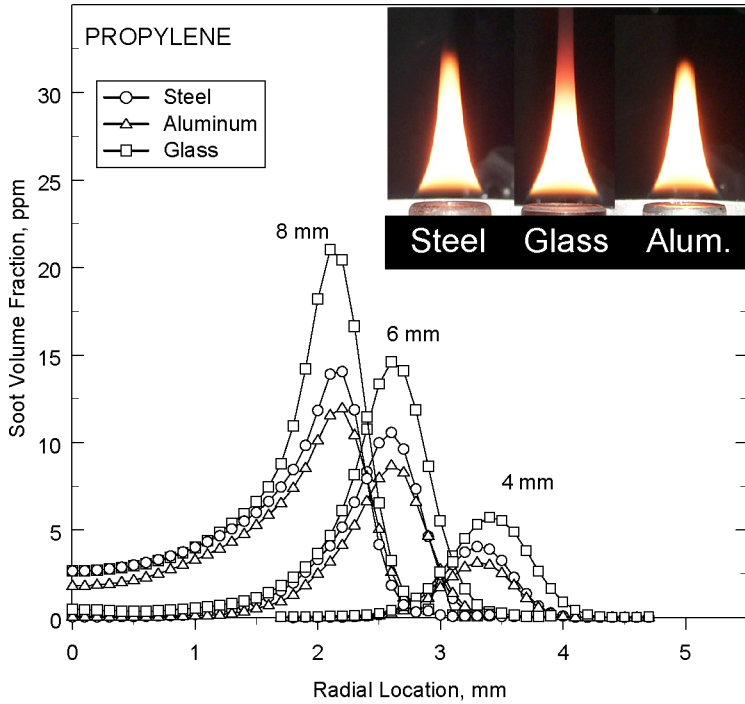
Fig. 3. Soot volume fraction profiles of propylene as a function of radial location in the flame at downstream locations of 4, 6, and 8 mm with three different fuel nozzle materials. The inset shows the photographs of the propylene flames with three different nozzle materials. The glass nozzle produces a sooting flame and soot escapes from the flame tip (middle photograph).
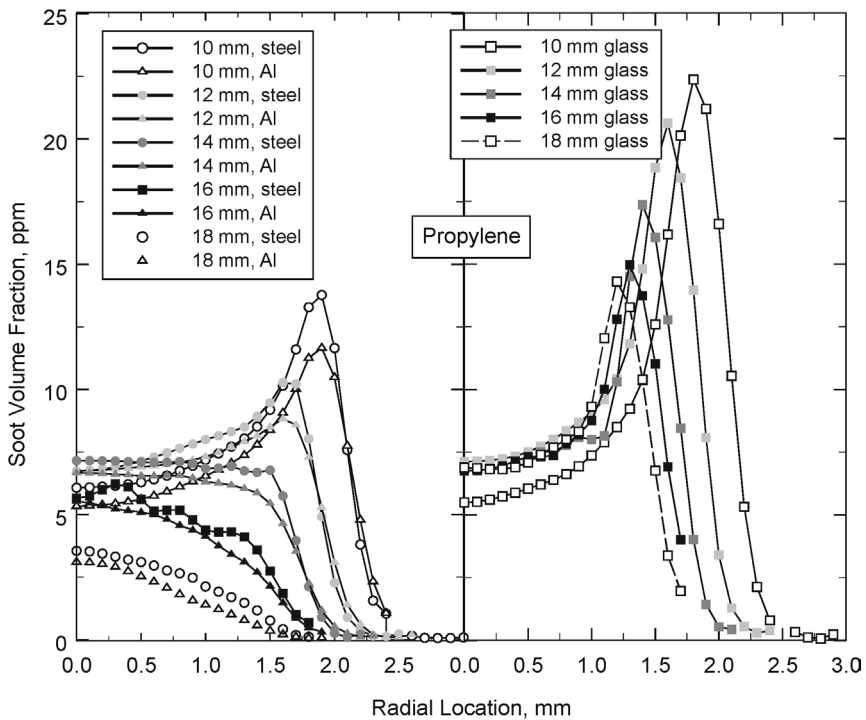


Fig. 4. Soot volume fraction profiles of propylene as a function of radial location in the flame at downstream locations of 10, 12, 14, 16, and 18 mm with three different fuel nozzle materials.
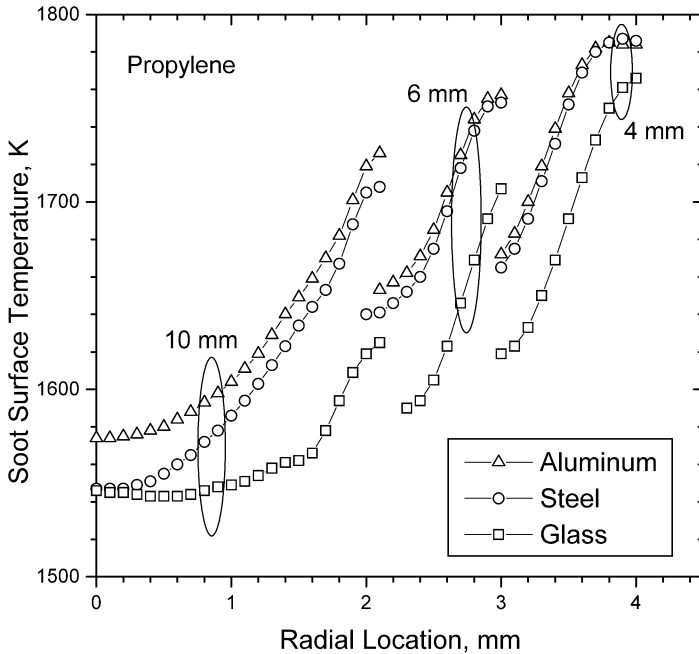
Fig. 5. Soot surface temperature profiles of propylene as a function of radial location in the flame at downstream locations of 4, 6, and 10 mm with three different fuel nozzle materials.
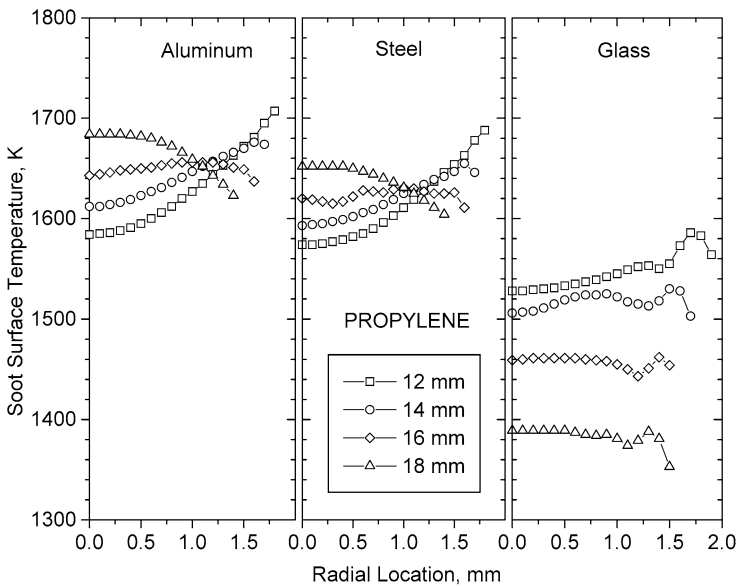


Fig. 6. Soot surface temperature profiles of propylene as a function of radial location in the flame at downstream locations of 12, 14, 16, and 18 mm with three different fuel nozzle materials.

The glass fuel nozzle heats the reactant gases more than the aluminum and steel, and thus the soot formation, which takes place through the pyrolysis of the fuel, is enhanced as the reactant temperatures are elevated [15] in the soot inception region lower in the flame.

Further, the radiative heat absorbed by the fuel nozzle is directly proportional the emissivity of the material. Glass, steel, and aluminum have emissivities about 0.9, 0.5, and 0.2, respectively [16], and their radiative heat gains are proportional to these values. Thus, higher emissivity and lower thermal conductiv-
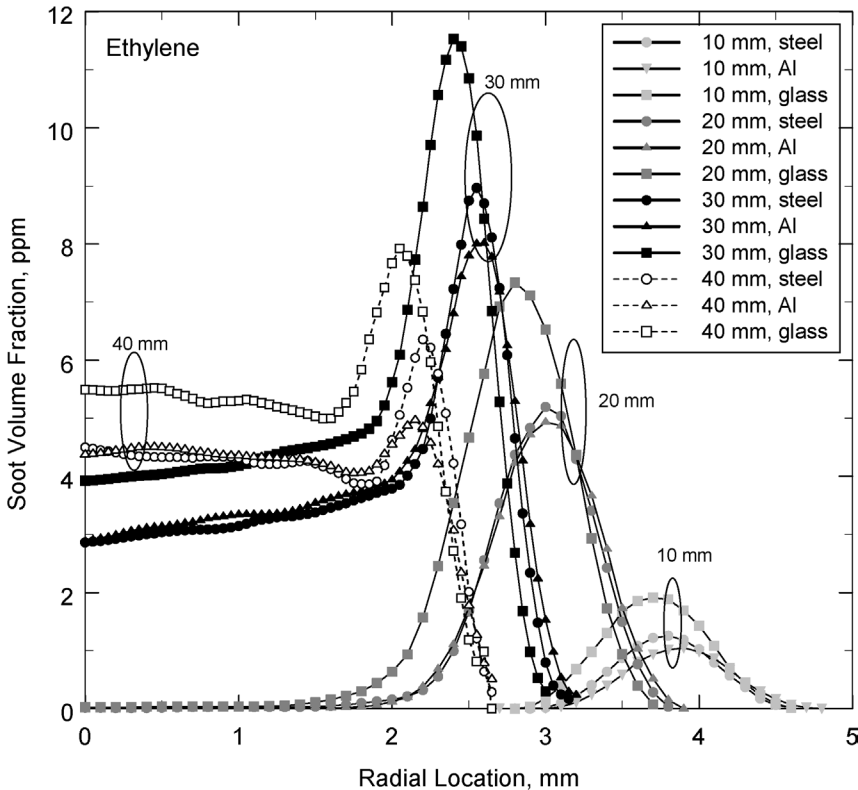
Fig. 7. Soot volume fraction profiles of ethylene as a function of radial location in the flame at downstream locations of 10, 20, 30, and 40 mm with three different fuel nozzle materials.

ity of the glass nozzle lead to the sooting behavior seen in Figs. 3 and 4.

The fuel nozzle outer surface temperatures as measured by thermocouples are shown in Fig. 1. The inner surface temperatures of the nozzles are expected to be much higher than these, especially for the glass nozzle (the inner surface temperatures were not measured because a thermocouple would disturb the fuel flow which would subsequently distort the whole flame). However, the nozzle outer surface temperatures shown in Fig. 1, when considered with the thermal diffusivities of the three materials, give a rough indication of the relative magnitudes of heat dissipation by axial conduction along the fuel pipe for the three different nozzles.

As a result of the foregoing discussion one would intuitively expect that the soot surface temperatures will be higher for the glass nozzle flame than for the other two metal nozzle flames. It should be noted that heat loss from the soot laden flames by soot radiation could be nontrivial and may account for 20 to 30% of the total chemical heat release depending on the soot concentration [17]. As a result of higher soot concentrations, the glass nozzle flame loses relatively more heat by radiation in the soot formation region

than the other two metal nozzle flames, and hence has lower soot surface (and gas) temperatures as shown in Figs. 5 and 6. As a consequence of significantly lower temperatures in the upper half of the flame, soot oxidation slows down and eventually stops, leading to soot escape from the tip of the flame of the glass fuel nozzle (inset in Fig. 3).

### 3.2. Ethylene flames

The soot concentration profiles of ethylene flames with different fuel nozzle materials display results similar to those of propylene. However, the difference between soot concentrations of the glass nozzle flame and the metal nozzle flames decreases with an increase in downstream distance (Fig. 7). At a 10 mm downstream location, the peak soot concentration of glass nozzle flame is about 80% higher than that of the aluminum nozzle, and this difference decreases to about 50% at a downstream location of 40 mm (Fig. 7). The soot concentration differences between different fuel nozzle material flames diminish by the time the flame tip is reached and all three nozzles produce flames burning just under smoke point con-
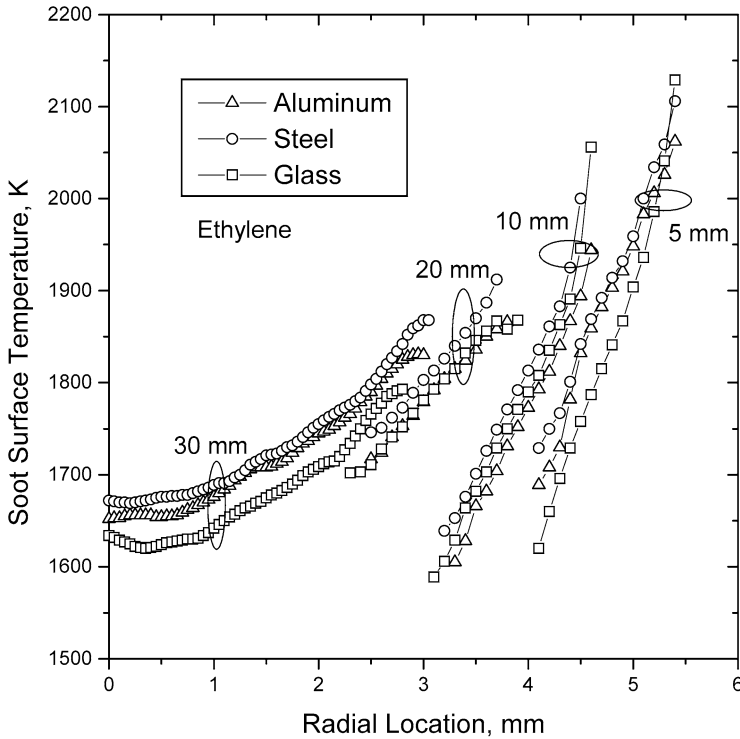
Fig. 8. Soot surface temperature profiles of ethylene as a function of radial location in the flame at downstream locations of 5, 10, 20, and 30 mm with three different fuel nozzle materials.

ditions and no soot escapes from the flames, contrary to the propylene flame with the glass fuel nozzle.

The ethylene flames of three different fuel nozzles show smaller differences in soot surface temperatures at downstream locations of 5, 10, and 20 mm (Fig. 8) than the corresponding propylene flames. This is expected because of the lower soot concentrations, and hence reduced radiative heat losses, in ethylene flames as compared to propylene flames. At flame heights beyond 30 mm, soot surface temperatures of the glass nozzle flame were lower than the metal nozzle flames by about 50 K. Soot surface temperature profiles of the aluminum and steel nozzle flames were almost identical.

These results with ethylene flames are in quantitative agreement with the limited results of Kent and Wagner [2]. They made the measurements by placing a 5 mm high glass ring on the brass fuel tube which was cooled with a water jacket thermostatically maintained at 40 °C. Their data consisted of integrated soot volume fraction along the flame height and the radial temperature profile at 5 mm above the burner rim with and without the glass ring.

It seems that the nozzle heating of the flame exerts a significant influence on the soot formation/oxidation and the temperature field of the whole flame in propylene and ethylene flames. The influence is more severe in the case of the smaller more highly sooting propylene flame. Whereas on the larger flame (ethylene) the influence is mainly in the lower half of the flame. In the upper half of the ethylene flame these effects are not as high as they are in propylene flames. It should also be noted that the radiative heat transfer to the fuel nozzle is greater for the propylene flame than the ethylene flame due to two factors: The soot concentrations are higher in the propylene flame, and due to the smaller height of the propylene flame the propylene fuel nozzle sees a larger viewing angle of radiation than the ethylene fuel nozzle.

Most recently, in studies related to soot formation under elevated pressures, it has been demonstrated that only small-size diffusion flames (less than 20 mm in height) can be stabilized at higher pressures [18,19]. Since the current work shows the nontrivial effect of nozzle material properties on flame structure, this concern should be taken into consideration in further measurements and simulations of laminar diffusion flames at high pressures.

### Acknowledgments

## References

[1] F.G. Roper, Combust. Flame 29 (1977) 219–234.
[2] J.H. Kent, H.G. Wagner, Combust. Sci. Technol. 41 (1984) 245–269.
[3] Ö.L. Gülder, Combust. Flame 88 (1992) 74–82.
[4] Ö.L. Gülder, Combust. Flame 92 (1993) 410–418.
[5] C.S. McEnally, A.M. Schaffer, M.B. Long, L.D. Pfefferle, M.D. Smooke, M.B. Colket, R.J. Hall, Proc. Combust. Inst. 27 (1998) 1497–1505.
[6] M.D. Smooke, C.S. McEnally, L.D. Pfefferle, R.J. Hall, M.B. Colket, Combust. Flame 117 (1999) 117–139.
[7] F. Liu, H. Guo, G.J. Smallwood, Ö.L. Gülder, Combust. Flame 125 (2001) 778–787.
[8] C.R. Kaplan, C.R. Shaddix, K.C. Smyth, Combust. Flame 106 (1966) 392–405.
[9] I.M. Kennedy, D.R. Rapp, R.J. Santoro, C. Yam, Combust. Flame 107 (1996) 368–382.
[10] D.R. Snelling, K.A. Thomson, G.J. Smallwood, Ö.L. Gülder, E.J. Weckman, R.A. Fraser, AIAA J. 40 (2002) 1789–1795.
[11] Ö.L. Gülder, D.R. Snelling, R.A. Sawchuk, Proc. Combust. Inst. 26 (1996) 2351–2357.
[12] C.J. Dasch, Appl. Opt. 31 (1992) 1146–1152.
[13] D.R. Snelling, K.A. Thomson, G.J. Smallwood, Ö.L. Gülder, Appl. Opt. 38 (1999) 2478–2485.
[14] E.R.G. Eckert, R.M. Drake, Heat and Mass Transfer, McGraw–Hill, New York, 1959, Appendix A.
[15] I. Glassman, Proc. Combust. Inst. 27 (1998) 1589–1596.
[16] M.F. Modest, Radiative Heat Transfer, McGraw–Hill, New York, 1993, Appendix B.
[17] G.G. Markstein, Proc. Combust. Inst. 22 (1988) 363–370.
[18] L.L. McKrain, W.L. Roberts, Combust. Flame 140 (2005) 60–69.
[19] K.A. Thomson, Ö.L. Gülder, E.J. Weckman, R.A. Fraser, G.J. Smallwood, D.R. Snelling, Combust. Flame 140 (2005) 222–232.